

Many-body theory of the electronic structures in ultrathin transition-metal films: bcc Co(001)

Changfeng Chen

*Department of Physics, University of Nevada, Las Vegas, Las Vegas, Nevada 89154**
and Physics Department and Materials Science Institute, University of Oregon, Eugene, Oregon 97403

(Received 6 August 1990)

An exact solution of a two-site crystal model with periodic boundary conditions, a two-layer {001} film with body-centered-cubic (bcc) crystalline structure, is presented for cobalt. The object is to study the many-body electronic structures of highly correlated metallic ultrathin epitaxial films. Surface effects and the confinement of the particle motion in an essentially two-dimensional layer are found to have an important influence on the electronic structures. A realistic local-density-approximation one-electron spectrum and an intrasite electron-electron interaction of full generality are used. The crystal field and the single-particle electronic structure in the bcc cobalt film are discussed. The many-body energy spectrum, the ground-state magnetization, the average magnetization and total electronic energy as a function of temperature, and the photoemission and inverse photoemission spectra are calculated. Some interesting many-body-effect-induced features are found and discussed. Physical conclusions about the many-body states in ultrathin bcc cobalt films are drawn.

I. INTRODUCTION

The understanding of the properties of transition metals presents the theoretical challenge of a full many-body problem. The magnitude of the Coulomb interaction between the d electrons in transition metals is close to, or in some cases even larger than, the d -band width. This strong electron-electron interaction invalidates the normal local-spin-density-approximation (LSDA) description¹⁻³ in some fundamental aspects. More careful treatment beyond LSDA to the interaction terms is required in order to obtain an appropriate theoretical description for such highly correlated systems. Among various many-body techniques, the recently developed periodic small-cluster approach⁴ (PSCA) has proved to be very good at determining spatially uniform and short-range properties of highly correlated systems.

In PSCA, a model Hamiltonian that explicitly includes band-structure effects and many-body interactions is solved exactly. The problem is made tractable by modeling the sample as a finite-size crystal with periodic boundary conditions. This is equivalent to solving exactly a many-body problem with integrals in momentum space restricted to a finite sampling. This technique of sampling only a few points in the Brillouin zone has been successfully used in one-electron calculations and in various problems, including some transition-metal systems,⁵⁻⁷ where local many-body effects are important.

In recent years, much attention has been attracted to fabricating and understanding the properties of ultrathin transition-metal films, due to their importance in both fundamental research and applications. Among them, the body-centered-cubic (bcc) phase of cobalt is an especially interesting example. Earlier experimental work⁸ on Cr/Co/Cr multilayer structures indicated that the cobalt film possesses the bcc crystalline structure, instead of its natural hexagonal-close-packed (hcp) structure. Most re-

cently, it has been reported^{9,10} that bcc thin-film structures are obtained when cobalt is epitaxially deposited on GaAs(110) and Fe(001) substrates, with the thickness of the film varying from a few atomic layers up to several hundred angstroms. Several band-structure and total-energy calculations¹¹⁻¹⁶ based on the local-density-approximation (LDA) have been reported for the bulk bcc cobalt phase. LDA calculations are very successful in explaining many properties of a large variety of materials, including some ground-state properties of transition metals. However, there are many-body effects that cannot be explained in this approach. This is particularly true when the full knowledge about the excited states is required. The PSCA is a suitable means for providing a full description beyond LDA for highly correlated systems, such as transition metals.

It is the purpose of this paper to present a many-body theory for ultrathin bcc cobalt films and pay special attention to the many-body-effect-induced features. In ultrathin-film structures, surface effects undoubtedly have an important influence on the properties of the system. It is expected that the many-body correlations will be stronger than those in bulk systems due to the reduction of the dimension of the system¹⁷ and may induce new features. In metallic cobalt, the Coulomb interactions between the d electrons are among the strongest in transition metals; this makes cobalt, particularly its ultrathin-film structure, an ideal candidate for the study of many-body effects in highly correlated itinerant magnetic systems.

This paper is arranged as follows. Section II presents the Hamiltonian and method of calculation. Section III contains the analysis of the many-body eigenvalue spectrum and thermodynamics, and Sec. IV shows the one-particle density of states that would be measured in photoemission and inverse photoemission experiments. The results are summarized in Sec. V. A brief account of this work has been reported previously.¹⁸

II. HAMILTONIAN AND METHOD OF CALCULATION

We take a two-site cluster, the smallest nontrivial bcc crystal, and apply periodic boundary conditions in a two-dimension plane to form an infinite two-layer slab in the [001] orientation. This is equivalent to sampling the γ point, the center of the surface Brillouin zone (SBZ). In this structure, each atom has only four nearest neighbors instead of eight as in a bulk bcc crystal. There are five d orbitals per atom per spin; in the presence of a cubic field, as in a bulk bcc crystal, these orbitals split into a triplet t_{2g} and a doublet e_g . In the present two-layer bcc structure the local environment for each atom is radically different from that in a bulk bcc crystal. As a result, the energies of all five d orbitals are shifted and split into more (three) energy levels. This crystal-field effect is one of the major features of the results obtained for the ultrathin-film structure.

The Hamiltonian contains both single- and two-particle terms:

$$H = \sum_{i,j;\mu,\nu;\sigma} t_{i\mu,j\nu} c_{i\mu\sigma}^\dagger c_{j\nu\sigma} + \sum_{i;\mu;\sigma} E_\mu c_{i\mu\sigma}^\dagger c_{i\mu\sigma} + \sum_{i;\mu,\nu,\lambda,\phi;\sigma,\sigma'} V_{\mu\nu\lambda\phi} c_{i\mu\sigma}^\dagger c_{i\nu\sigma'}^\dagger c_{i\lambda\sigma} c_{i\phi\sigma}. \quad (2.1)$$

Here i, j ($=1,2$) label atoms in the cluster; μ, ν, λ, ϕ ($=1,2,3,4,5$) label the five d orbitals; σ, σ' are spin indices. The single-particle hopping terms are parametrized according to the Slater-Koster scheme.¹⁹ The parameters for cobalt were initially taken from Victora's thesis,²⁰ and then adjusted to reproduce, in the absence of any interactions, the calculated paramagnetic LDA band structure at selected points in the Brillouin zone. Note that the two-atom cluster allows for only nearest-neighbor hopping; in the restricted crystal the second-nearest neighbor of an atom is identical to itself. The intra-atomic Coulomb interactions $V_{\mu\nu\lambda\phi}$ most generally allowed by atomic symmetry²¹ are used. They include a direct Coulomb integral U , an average exchange integral J , and an exchange anisotropy dJ . The intra-atomic interaction is the dominant contribution.²² The next-largest contribution is the nearest-neighbor Coulomb term, which makes a constant contribution in the cluster and may be neglected. The value of U is chosen, for the bulk bcc cobalt, to be 6.6 eV to reproduce the correct ground-state magnetization using a scaling relation between the bcc iron and bcc cobalt results.²⁰ Other interaction parameters are set in the ratios $U:J:dJ=58:8:1$ based on the consideration of the constraints imposed by the atomic data and the screening effect in metal. (The results are insensitive to exact values of these ratios in our calculation.) It is expected that the value of U will be enhanced at surfaces due to band narrowing. However, we find that it does not affect our results in any fundamental way when the value of U increases by a few eV from its bulk value.

It is clear that the crystal-field effect is, in the two-layer structure, quite different from that of the bulk, because the atom in these "surface" layers have fewer neighbors. A straightforward calculation shows that the energy shifts of the five d orbitals caused by the crystal-field

effect in the thin-film case can be written as

$$\Delta E_\alpha = -(16/15)d_{1n} + (4/15)d_{2n}, \quad (2.2a)$$

$$\Delta E_\beta = -(16/15)d_{1n} + (44/15)d_{2n}, \quad (2.2b)$$

$$\Delta E_\gamma = \Delta E_\delta = \Delta E_\epsilon = (32/45)d_{1n} - (16/15)d_{2n}, \quad (2.2c)$$

where the subscripts $\alpha, \beta, \gamma, \delta$, and ϵ refer to the five d orbitals of symmetry $r^2-3z^2, x^2-y^2, xy, yz$, and xz , respectively. The values of d_{1n} and d_{2n} , which are the contributions to the energy shifts from each of the first and second neighbors, are determined by the bulk crystal-field analysis and the assumption⁶

$$d_{2n}/d_{1n} = (dd\sigma)_2/(dd\sigma)_1 \quad (2.3)$$

where $(dd\sigma)_1$ and $(dd\sigma)_2$ are the Slater-Koster tight-binding parameters. Now the position of the d levels of the two-layer cobalt film can be obtained easily. They are listed together with the other Hamiltonian parameters in Table I.

Metallic cobalt in the hcp phase has a magnetic moment of $1.72\mu_B$ (μ_B is the Bohr magneton) per atom.²³ Experimental⁸ and theoretical²⁴ estimates show that cobalt in bcc phase has a magnetic moment of similar size. Because of the saturation of magnetization in metallic cobalt,²⁵ its value only has a very slight increase at surfaces. We consider a cobalt ground state consisting of two holes per atom, i.e., four holes in the cluster. It allows a maximum magnetization of $2.00\mu_B$ per atom, which is very close to the estimates mentioned above. Only d states are explicitly included in the calculation. The s -like conduction band can be treated as an electron reservoir which has "absorbed" four electrons; the hybridization between the conduction and d electrons is effectively taken into account by adjusting d levels to fit the all-electron band-structure results.

With five d orbitals per atom per spin, there are 20 orbitals in the two-atom cluster. Simple combinatorial arguments yield 4845 states for four holes in the cluster. The photoemission process introduces a fifth hole, yielding 15 540 final states. Inverse photoemission removes a hole, leaving three in the cluster, for a total of 1140 final states. Clearly, we have a large manifold of many-body states in the cluster. The space and spin symmetries inherent in the Hamiltonian must be exploited in order to diagonalize the complete many-body matrices. First, to

TABLE I. Hamiltonian parameters (in units of eV).

| | |
|--------------|--------|
| $(dd\sigma)$ | -0.681 |
| $(dd\pi)$ | 0.449 |
| $(dd\delta)$ | -0.080 |
| E_α | 9.739 |
| E_β | 10.440 |
| E_γ | 10.177 |
| E_δ | 10.177 |
| E_ϵ | 10.177 |
| U | 6.6 |
| J | 0.943 |
| dJ | 0.118 |

TABLE II. The character table of the two-atom-cluster nonsymmorphic space group for the two-layer {001} bcc film. There is only one translation (the identical translation) in the cluster. There are two fourfold and one twofold rotations around the z axis ($C_{4z}, C_{4z}^2, C_{4z}^{-1}$). There are also four twofold screw axes parallel to the x - y plane (their rotational part is formed by one of the following four point operations: $C_{2x}, C_{2y}, C_{2d}, C_{2d'}$). The symbol τ stands for the vector that connects the two atoms in the cluster. Note that τ is *not* a translational operation in the system.

| | 1 | 1 | 2 | 2 | 2 |
|------------|-----|------------|-----------------------|------------------------|-------------------------|
| | E | C_{4z}^2 | C_{4z}, C_{4z}^{-1} | $C_{2x}, C_{2y}; \tau$ | $C_{2d}, C_{2d'}; \tau$ |
| γ_1 | 1 | 1 | 1 | 1 | 1 |
| γ_2 | 1 | 1 | -1 | 1 | -1 |
| γ_3 | 1 | 1 | 1 | -1 | -1 |
| γ_4 | 1 | 1 | -1 | -1 | 1 |
| γ_5 | 2 | -2 | 0 | 0 | 0 |

tal spin in the cluster is a good quantum number. For the case of four holes in the cluster, there are 825 singlets, 990 triplets, and 210 quintets. For the case of five (three) holes in the cluster, there are 1512 (0) sextets, 7392 (480) quadruplets, and 6600 (660) doublets. Furthermore, space-group decomposition reduces the sizes of matrices in a very efficient way.

The space group for the two-layer {001} bcc film is a nonsymmorphic one, of order 8. It possesses five irreducible representations with the following degeneracies: γ_1 ($d=1$), γ_2 ($d=1$), γ_3 ($d=1$), γ_4 ($d=1$), and γ_5 ($d=2$). Table II lists the character table of the space group of the two-layer {001} bcc film. With a complete set of matrices that transform according to these irreducible representations, it is possible to project out sets of symmetrized basis states.²⁶ Since the representations cannot mix, this is equivalent to a block diagonalization of the Hamiltonian. In the case of four holes in the cluster, the largest block is of order 252, a considerable reduction from the original matrix of order 4845. The largest blocks for five and three holes in the cluster²⁷ are of order 820 and 82, respectively. The various block sizes are shown in Table III. The solutions obtained by diagonalizing these blocks are exact solutions of the full Hamiltonian for the cluster.

III. MANY-BODY EIGENVALUE SPECTRUM AND THERMODYNAMICS

The many-body eigenvalue spectrum is usually quite complicated. Our results may be understood by making a Hubbard-model-like interpretation in which the single-

particle levels are split by the exchange interaction J into single-particle majority-spin and minority-spin levels.²⁸ This is, of course, only an approximate picture, since in the full many-body approach configuration interaction mixes all one-particle levels; nevertheless, it is very useful in understanding the physics in the problem and making some qualitative analysis before performing the full many-body calculations.

The one-particle energy levels of the two-layer bcc cobalt film are presented in Table IV. In this case, the highest one-electron level is γ_2 , which is nondegenerate and can accommodate one hole of each spin. The next highest level is a threefold-degenerate one, of symmetries γ_2 and γ_5 , which can accommodate three holes of each spin. The next level is again a nondegenerate one of γ_1 symmetry. When the Coulomb interaction is turned on, the spin states are split by approximately J , which is sufficient to bring the top γ_2 majority-spin level below the γ_1 minority-spin level. (The other levels are too far away to matter.)

From the above picture, one can see that the four holes in the cluster should go to the γ_2 and γ_2/γ_5 manifold minority-spin levels, yielding a fully saturated ferromagnetic state with a spin per atom of 2. This is consistent with our actually calculated ground state of $^5\gamma_4$ symmetry, which represents well the saturated magnetization observed in bulk and surface cobalt systems.

The density of many-body states (MBDOS) is the best way to show the spectrum of energy eigenvalues of the Hamiltonian. At each eigenvalue,²⁹ a peak of weight equal to the degeneracy at that energy is plotted. In a

TABLE III. Sizes of the blocks of the various representations for the two-layer {001} bcc film space group.

| | | γ_1 | γ_2 | γ_3 | γ_4 | γ_5 |
|-------|-------------------|------------|------------|------------|------------|------------|
| $N=3$ | $J = \frac{3}{2}$ | 14 | 14 | 14 | 14 | 32 |
| | $J = \frac{1}{2}$ | 41 | 42 | 41 | 42 | 82 |
| $N=4$ | $J=2$ | 31 | 27 | 21 | 27 | 52 |
| | $J=1$ | 117 | 121 | 127 | 121 | 252 |
| | $J=0$ | 119 | 106 | 94 | 106 | 200 |
| $N=5$ | $J = \frac{5}{2}$ | 34 | 32 | 34 | 32 | 60 |
| | $J = \frac{3}{2}$ | 230 | 230 | 230 | 230 | 464 |
| | $J = \frac{1}{2}$ | 414 | 416 | 414 | 416 | 820 |

TABLE IV. One-particle energy levels (in units of eV) for the two-layer bcc cobalt film structure. The degeneracies shown here are per spin.

| Energy | Symmetry | Degeneracy |
|--------|----------------------|------------|
| 11.528 | γ_2 | 1 |
| 10.829 | γ_2, γ_5 | 3 |
| 10.827 | γ_1 | 1 |
| 9.525 | γ_4, γ_5 | 3 |
| 9.352 | γ_4 | 1 |
| 8.651 | γ_3 | 1 |

finite system, this results in a discrete set of spikes, which we have broadened artificially into Gaussians of 0.1 eV half-width, at half-maximum. Figure 1 shows the MBDOS of the two-layer cobalt film.

The PSCA can provide the full description of both eigenvalues and eigenstates, allowing one to compute various correlation functions. These correlations may be plotted as functions of temperature in the following way:

$$\langle A(T) \rangle = \sum_i \langle i | A | i \rangle \exp \left[-\frac{E_i}{k_B T} \right], \quad (3.1)$$

where A is the correlation function, $|i\rangle$ the appropriately normalized eigenstates with eigenvalue E_i , k_B the Boltzmann constant, and T the temperature. In this way, one can obtain the knowledge of the thermodynamics of the systems in a full many-body picture.

Here we only give the results of two most obvious functions of the system, namely the total electronic energy E and the magnitude of the total spin square S^2 . Results are shown in Fig. 2. Any desired correlation as a function of temperature can be obtained from Eq. (3.1); but, of course, only those of uniform and short-range character are reliable, due to the limitation of the present approach.

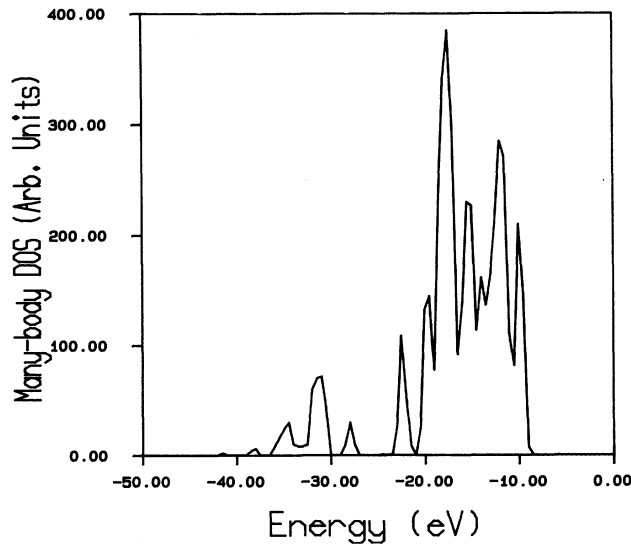


FIG. 1. The eigenvalue spectrum (density of many-body states) for the two-layer bcc Co(001) film.

IV. PHOTOEMISSION AND INVERSE PHOTOEMISSION

Photoemission and inverse photoemission measurements provide a useful probe of the electronic structure in highly correlated systems. The physical process involved is intrinsically short ranged. Therefore it should be well described in the PSCA.

The photoemission spectrum (PES) is defined as

$$F_{\text{PE}}(\epsilon, \mu\sigma) = \sum_k |\langle \nu^{(k)} | c_{\mu\sigma} | \psi_0 \rangle|^2 \delta(\epsilon - \epsilon^{(k)} + \epsilon_0), \quad (4.1)$$

where $|\nu^{(k)}\rangle$ is the k th eigenstate in the five-hole final-state manifold of the cluster, $|\psi_0\rangle$ is the four-hole ground state, and $\epsilon^{(k)}$ and ϵ_0 are the corresponding eigenvalues. The operator $c_{\mu\sigma}$ destroys an electron or, equivalently,

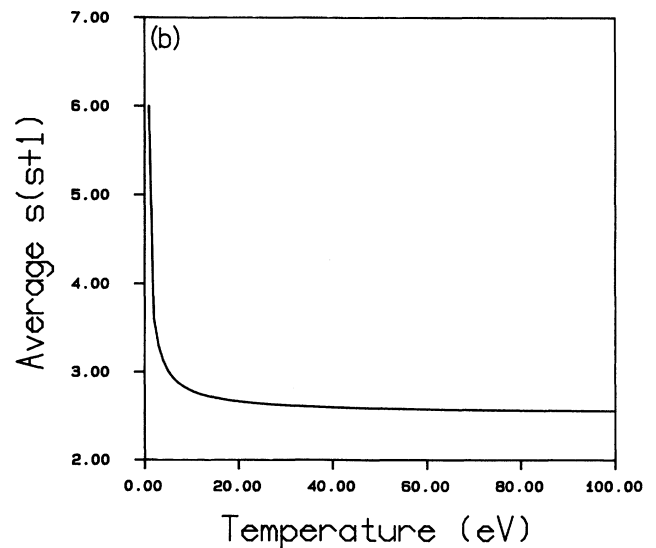
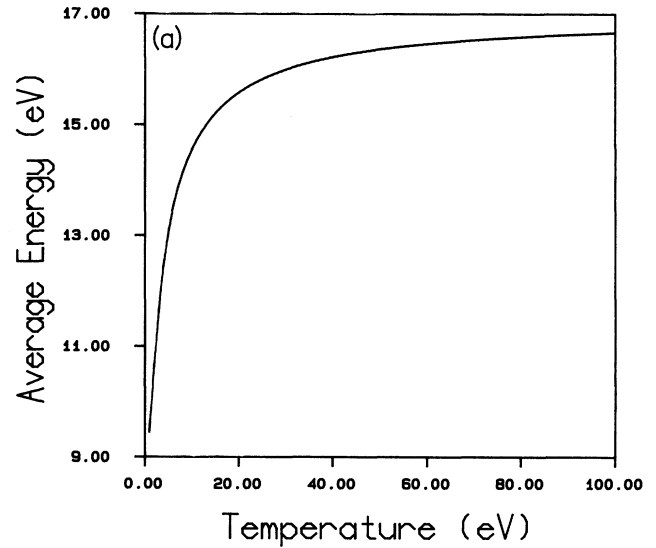


FIG. 2. The thermodynamic average of the total electronic energy and the total spin square S^2 of the two-layer bcc Co(001) film.

creates a hole on the orbital μ (μ runs over the 10 d orbitals in the cluster) with spin σ in the ground state. From Eq. (4.1) one can obtain angle-, spin-, energy-resolved, as well as fully integrated, PES results. The inverse photoemission spectrum (IPES) is similarly defined as

$$F_{\text{IPE}}(\varepsilon, \mu\sigma) = \sum_k |\langle \xi^{(k)} | c_{\mu\sigma}^\dagger | \psi_0 \rangle|^2 \delta(\varepsilon - \varepsilon^{(k)} + \varepsilon_0), \quad (4.2)$$

where $\xi^{(k)}$ is the k th eigenstate in the three-hole final-state manifold with eigenvalue $\varepsilon^{(k)}$.

Shown in Fig. 3 are the fully integrated PES and IPES results. They should be compared with normal-emission valence-band PES and IPES of ultrathin bcc cobalt films. The spin-resolved PES has been reported previously,¹⁸ and should be compared with spin-sensitive PES experimental data. For purposes of comparison, we have also computed PES and IPES in the single-particle picture for the same model, which are easy to obtain from the following calculated one-particle “density” peak positions with the corresponding degeneracies (energies are measured in eV from the Fermi energy): 0.000 (1), -0.699 (3), -0.701 (1), -2.003 (3), -2.176 (1), and -2.877 (1). Results are presented in Table V. A detailed analysis of our results yields the following conclusions.

(i) There is a pronounced band (projected onto the γ point, same below) narrowing due to the presence of the surfaces. LDA results give a bandwidth of 4.5 eV for the (artificial) bulk bcc cobalt. It is reduced to 2.9 eV in the two-layer thin-film structure. The band is further narrowed by many-body correlation effects by an amount of 0.5 eV.

(ii) There are three large-weighted and well-resolved “satellite peaks” (at energies $E < E_b$, E_b is the bottom of the band predicted by LDA calculations) in the spectra. The first one is immediately below E_b and is separated from the closest “main-line” ($E > E_b$) peak by 0.5 eV; the second one is very broad, centered around 5.5 eV below the Fermi level E_F ; the third is at 10.0 eV below E_F . It should not be difficult to detect them in a high-resolution photoemission measurement. This behavior has not been seen in any other known transition-metal systems. This is also quite different from the (artificial) bulk bcc cobalt results,³⁰ where satellite peaks are weak and not well resolved. For a long time, metallic nickel has been considered the only itinerant magnetic system showing a strong satellite peak in the photoemission spectra. Satellite peaks in the photoemission spectra of other transition-metal systems are normally weak and sometimes even debatable.³¹ The ultrathin bcc cobalt film is a possible candidate that will show strong satellite (multi-) peaks in photoemission spectra.

(iii) In the many-body approach, configuration interaction mixes all single-particle energy levels. A full many-body picture is necessary to understand the photoemission results. In metallic cobalt, there are more holes per atom than that in metallic nickel. This makes the correlation behavior of the holes in the cobalt films more complicated. Table VI shows the spectrum weights projected onto the states belonging to various irreducible representations. Both sets of the results calculated in a single-particle and a full many-body approach are presented. It

can be seen that the many-body results are *qualitatively* different from the single-particle results. The γ_2 states are partly above the Fermi level in LDA band-structure results; this is responsible for the small PES weight found for the γ_2 states in the single-particle picture. The pronounced increase of the PES weight of γ_2 states in our many-body calculation indicates that the energy levels nominally “above the Fermi level” are now occupied with non-negligible probability. Once again, this is purely a many-body effect, which is important in determining

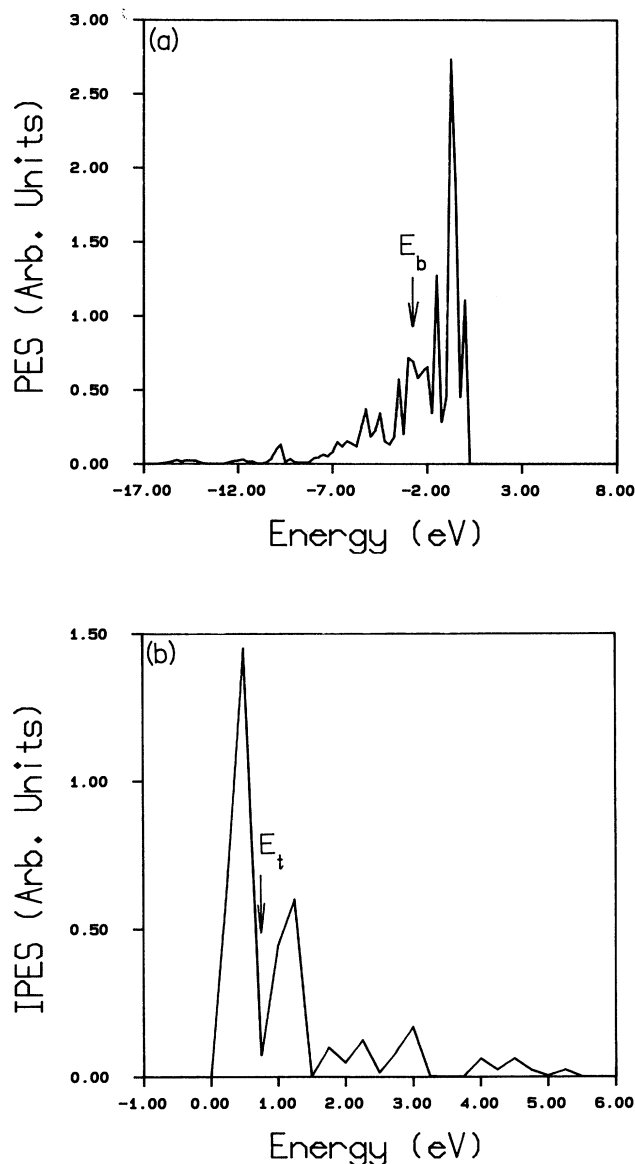


FIG. 3. The calculated normal-emission valence-band (a) photoemission spectrum (PES) and (b) inverse photoemission spectrum (IPES) of the two-layer bcc Co(001) film. The locations of the lowest and highest single-particle state at the center of the two-dimensional Brillouin zone in the d band according to LDA band-structure calculations are denoted by E_b and E_t , respectively.

TABLE V. Photoemission and inverse photoemission peaks in the single-particle picture.

| Symmetry | Peak energy (eV) | Peak weight |
|-----------------------|------------------|-------------|
| Inverse photoemission | | |
| γ_2, γ_5 | 0.000 | 1 |
| γ_2 | 0.669 | 1 |
| Photoemission | | |
| γ_2, γ_5 | 0.000 | 2 |
| γ_1 | -0.002 | 1 |
| γ_4, γ_5 | -1.304 | 3 |
| γ_4 | -1.477 | 1 |
| γ_3 | -2.178 | 1 |

electronic properties of the system. The drastic deviation of the projected spectrum weights from single-particle results has not been seen before for any other transition-metal systems. This qualitative deviation is a new feature observed here in the ultrathin bcc cobalt film, where the particles with strong Coulomb interactions are essentially confined in a two-dimensional plane.

(iv) The configurational interaction also brings the states nominally below the Fermi level up to the Fermi level. In our calculated photoemission spectra, states of symmetry γ_3 , which are at the bottom of the band according to the LDA calculation, not only mix in at the Fermi level, but also give the dominant contribution there. This is again *qualitatively* different from the “mix-in” effect observed in other transition-metal systems, where the mix-in contributions are never dominant.

(v) The exchange splitting in the main-line part of the spectra is quite small; the average exchange splitting throughout the energy range $E_b < E < E_F$ is less than 0.35 eV. However, the exchange splitting in the satellite part is fairly large, corresponding to a strong many-body interaction.

(vi) The overall calculated relative spin polarization of the photoemission spectra

$$(I_+ - I_-)/(I_+ + I_-),$$

where I_+ and I_- are the total intensities of the majority- and minority-spin states, is 25% in the majority-spin orientation. However, it is not evenly distributed. The peaks in the main-line part close to the Fermi level have a very weak (<10%) spin polarization, while those at the bottom of the main-line part and most of the satellite part

TABLE VI. The photoemission and inverse photoemission spectrum weights projected onto the states belonging to various irreducible representations. Both sets of the results calculated in the single-particle and many-body approach are listed.

| | Single-particle results | | Many-body results | |
|------------|-------------------------|------|-------------------|------|
| | PES | IPES | PES | IPES |
| γ_1 | 2.00 | 0.00 | 4.14 | 0.29 |
| γ_2 | 1.00 | 3.00 | 1.99 | 0.14 |
| γ_3 | 2.00 | 0.00 | 2.89 | 0.99 |
| γ_4 | 4.00 | 0.00 | 1.38 | 0.69 |
| γ_5 | 7.00 | 1.00 | 5.60 | 1.89 |

have a very high (up to 100%) spin polarization in the majority-spin orientation. This high spin polarization of the peaks in the spectra should be measured in a spin-resolved photoemission experiment.

(vii) Similar to the PES results discussed in (iii), we have also calculated the projected IPES weights onto various irreducible representations. Both sets of the results calculated in a single-particle and a full many-body approach are presented in Table VI together with the PES results. The drastic difference of the many-body results from those in the single-particle picture is demonstrated even more clearly than those in the PES results. Three nominally “filled” electronic energy levels with *zero* IPES projection weight are now “occupied” by holes with significant probability, yielding the pronounced IPES projection weights.

(viii) The ground state of the neutral cluster is a fully saturated ferromagnetic state, i.e., all the holes are in the minority-spin levels. An electron cannot be absorbed unless there is already a hole there. Therefore one should expect that all the IPES spectra are fully polarized in the minority-spin orientation. This is indeed the case of our calculated results shown in Fig. 3(b).

V. CONCLUSIONS

The electronic structures of a highly correlated ultrathin epitaxial transition-metal film, a bcc Co(001) dilayer, have been studied in an exactly soluble many-body periodic small-cluster approach. This approach incorporates both band-structure effects and many-body correlations on an equal footing. No perturbation theory was employed. The model is based on, but goes beyond, the local-density-approximation band-structure results; the solution can provide accurate and detailed information about some important properties, particularly those induced by strong local many-body correlations.

It is found that crystal-field effects and the associated change in the single-particle electronic structure play an important role in determining the many-body electronic structures. Since our approach can provide the full description of both the eigenvalues and eigenstates for the ground state as well as excited states, it is possible to determine any desired (uniform and short-range) correlation functions and the thermodynamics of the system in a full many-body picture.

Our exact many-body calculation of the photoemission and inverse photoemission spectra of the two-layer bcc Co(001) film has revealed some interesting new features. The most striking one is that the many-body correlation effects in the ultrathin bcc cobalt films, where particles are essentially confined in two dimensions, are strongly enhanced and lead to a *qualitative* deviation of the symmetry-projected spectrum weight distribution from the single-particle results, a phenomenon never observed in any other transition-metal systems. It is shown that ultrathin cobalt films could be the first example in magnetic transition-metal systems to have strong well-resolved satellite (multi-) peaks with large exchange splittings and high spin polarizations. This result suggests that ultrathin cobalt films may serve as a model system in

the study of the dimensional dependence of the many-body correlation effects in highly correlated electronic systems. Surface-sensitive, normal-emission valence-band photoemission and inverse photoemission experiments should be able to test our results. The results reported here should be insensitive to the thickness of the film in a reasonable range (e.g., 1–3 atomic layers). Some slight quantitative changes are expected as the thickness varies (e.g., when the film becomes thinner or thicker, the intensity of the satellite peaks are expected to increase or decrease, and the peak positions are expected to move toward higher or lower binding energy). However, our conclusion should not be affected in any fundamental way. Further work will be carried out to study the

influence of various substrates on the electronic and magnetic properties of ultrathin cobalt films; however, it is expected that it will not change the main conclusions reported here as long as the film-substrate coupling is not very strong.

ACKNOWLEDGMENTS

It is a pleasure to thank Professor T. W. Mossberg for generously providing the computer facilities used for the numerical calculations in this work. This research was partly supported by University of Nevada, Las Vegas. Partial support by the National Science Foundation under Grant No. DMR-88-19302 is gratefully acknowledged.

*Present address.

- ¹C. S. Wang, B. N. Klein, and H. Krakauer, *Phys. Rev. Lett.* **54**, 1852 (1985).
²J. Chen, D. Singh, and H. Krakauer, *Phys. Rev. B* **38**, 12 834 (1988).
³E. Di Fabrizio, G. Mazzone, C. Petrillo, and F. Sacchetti, *Phys. Rev. B* **40**, 9502 (1989).
⁴L. M. Falicov, in *Recent Progress in Many-Body Theories*, edited by E. Pajanne and R. Bishop (Plenum, New York, 1988), Vol. I, p. 275, and references therein.
⁵R. H. Victora and L. M. Falicov, *Phys. Rev. Lett.* **55**, 1140 (1985); E. C. Sowa and L. M. Falicov, *Phys. Rev. B* **35**, 3765 (1987).
⁶C. Chen and L. M. Falicov, *Phys. Rev. B* **40**, 3560 (1989).
⁷C. Chen, *Phys. Rev. B* **41**, 1320 (1990); **41**, 5031 (1990).
⁸R. Walmsley, J. Thompson, R. M. White, and T. H. Geballe, *IEEE Trans. Magn.* **MAG-19**, 1992 (1983).
⁹Y. U. Idzerda, W. T. Elam, B. T. Jonker, and G. A. Prinz, *Phys. Rev. Lett.* **62**, 2480 (1989).
¹⁰H. Li and B. P. Tonner, *Phys. Rev. B* **40**, 12 241 (1989).
¹¹D. Bagayoko, A. Ziegler, and J. Callaway, *Phys. Rev. B* **27**, 7046 (1983).
¹²G. A. Prinz, *Phys. Rev. Lett.* **54**, 1051 (1985).
¹³V. L. Moruzzi, P. M. Marcus, K. Schwarz, and P. Mohn, *J. Magn. Magn. Mater.* **54–57**, 955 (1986).
¹⁴B. I. Min, T. Oguchi, and A. J. Freeman, *Phys. Rev. B* **33**, 7852 (1986).
¹⁵J. I. Lee, C. L. Fu, and A. J. Freeman, *J. Magn. Magn. Mater.* **62**, 93 (1986).
¹⁶G. A. Prinz, E. Kisker, K. B. Hathaway, K. Schroder, and K.-H. Walker, *J. Appl. Phys.* **57**, 3024 (1985).
¹⁷The film-substrate coupling usually tends to make the system more “bulklike.” However, one can choose proper substrates (e.g., semiconductors such as GaAs or some insulating materials) to minimize the coupling between the *d* electrons in the cobalt films and the electrons in the substrate materials. Actually, even at the semi-infinite cobalt surfaces, where the coupling is “perfect,” there is a magnetization enhancement, indicating a more localized character of the *d* electrons and

thus a stronger many-body correlation therein.

- ¹⁸C. Chen, *Phys. Rev. Lett.* **64**, 2176 (1990).
¹⁹J. C. Slater and G. F. Koster, *Phys. Rev.* **94**, 1498 (1954); corrected and extended to include *f* electrons by R. R. Sharma, *Phys. Rev. B* **19**, 2813 (1979).
²⁰R. H. Victora, Ph.D. thesis, University of California, Berkeley, 1985.
²¹M. Tinkham, *Group Theory and Quantum Mechanics* (McGraw-Hill, New York, 1964).
²²C. Herring, in *Magnetism: A Treatise on Modern Theory and Materials*, edited by G. T. Rado and H. Suhl (Academic, New York, 1966), Vol. 4.
²³C. Kittel, *Introduction to Solid State Physics*, 5th ed. (Wiley, New York, 1976), p. 465.
²⁴R. H. Victora and L. M. Falicov, *Phys. Rev. B* **30**, 259 (1984).
²⁵R. H. Victora and L. M. Falicov, *Phys. Rev. B* **30**, 3896 (1984).
²⁶A. W. Luehrmann, *Adv. Phys.* **17**, 1 (1968).
²⁷Since the ground state in the present case is a fully saturated ferromagnetic state ($J=2$), the final state in the photoemission process can only be either $J=\frac{5}{2}$ or $\frac{3}{2}$, states, i.e., $J=\frac{1}{2}$ states never get involved. This means that the largest Hamiltonian matrix one has to deal with here is of order 464 for the states of $^4\gamma_5$ symmetry, instead of the one of $^2\gamma_5$ symmetry, which is of order 820.
²⁸Any use of words “majority” or “minority” in the context of the spin orientation of an energy level refers to electronic spin, not to the spin of the hole. In particular, if the spin orientations of all holes in the ground state are the same, these holes are in minority-spin states.
²⁹The MBDOS should not be confused with the usual single-particle DOS; here the eigenvalues are the energies of many-body states rather than single-particle excitation energies.
³⁰C. Chen (unpublished).
³¹D. Chandesaris, J. Lecante, and Y. Petroff, *Phys. Rev. B* **34**, 8971 (1986); H. Kato, T. Ishii, S. Masuda, Y. Harada, T. Miyano, T. Komeda, M. Onchi, and Y. Sakisaka, *ibid.* **34**, 8973 (1986).